



Synthesis of a Novel Benzimidazole Moiety-Appended Schiff Base Derivative: Fluorescence and Chemosensor Study

Pinar Sen^{a,b,*}, S. Zeki Yildiz^a, Necmi Dege^c, Göknur Yasa Atmaca^d,
Ali Erdogmus^d, Mustafa Dege^e

^aSakarya University, Faculty of Arts and Sciences, Department of Chemistry, 54187, Sakarya, Turkey

^bCentre for Nanotechnology Innovation, Department of Chemistry, Rhodes University, Grahamstown, 6140, South Africa

^cOndokuz Mayıs University, Faculty of Arts and Sciences, Department of Physics, 55139 Samsun, Turkey

^dDepartment of Chemistry, Yildiz Technical University, 34210 Esenler, Istanbul, Turkey

^eSpraying Systems Company, Kaya Aldoğan sok. No: 3/3 34394 Zincirlikuyu Şişli-İstanbul, Turkey

Abstract: In this study, we synthesized a novel benzimidazole-based Schiff base; (E)-4,4'-methylenebis(2-((E)-(((1H-benzo[d]imidazol-2-yl)methyl)imino)methyl)phenol) (**3**) was synthesized by the condensation of 5,5'-methylenebis(2-hydroxybenzaldehyde) (**1**) and (1H-benzo[d]imidazol-2-yl)methanamine.HCl salt (**2**). This Schiff base derivative was reported for the first time and fully characterized by common spectroscopic techniques. Absorption and fluorescence spectroscopy were recorded to determine the sensing ability of **3** towards metal ions. Selectivity to Zn²⁺ ion among studied other cations was detected. The crystal structure of **2**, C₈H₁₃Cl₂N₃O, has been determined by single crystal X-ray diffraction method. The crystal structure of the title compound, C₈H₁₁N₃²⁺·2(Cl⁻)·H₂O, consists of an organic 1H-benzoimidazol-3-ium (C₈H₁₁N₃²⁺) cation, an inorganic 2(Cl⁻) anion and one water (H₂O) molecule. In the cation of studied compound, C₈H₁₁N₃²⁺, the benzimidazole ring is almost planar with a maximum deviation of -0.012 (3) Å. The molecule crystallized in the monoclinic structure and the space group P2₁/c. The crystalline stacking structure is stabilized by intramolecular N-H...Cl, N-H...O, the intermolecular N-H...Cl hydrogen bond interactions connection the molecules into a two dimensional network and between anions and the water molecules. π-π interaction between benzimidazole rings [centroid-centroid lengths = 3.4642 (2) Å, 3.5309 (2) Å and 3.5527 (2) Å] may further stabilize the structure.

Keywords: Synthesis, benzimidazole derivative, Schiff base, Single crystal, X-ray crystallography, Crystal structure, Fluorescence property.

Submitted: November 05 ,2018. **Accepted:** December 12, 2018.

Cite this: Sen P, Yildiz S, Dege N, Yasa Atmaca G, Erdogmus A, Dege M. Synthesis of a Novel Benzimidazole Moiety-Appended Schiff Base Derivative: Fluorescence and Chemosensor Study. JOTCSA. 2019;5(3):1375-88.

DOI: <http://dx.doi.org/10.18596/jotcsa.478665>.

***Corresponding Author, E-mail:** sen_pinar@hotmail.com.

INTRODUCTION

Benzimidazole derivatives have aroused interest in recent years. Researches on this heterocyclic compounds have been carried on increasingly (1). Benzimidazole derivatives are widely used due to their biological activities such as anticancer, antiulcers,

antifungals, anti-inflammatory agents, antimycobacterials, and antioxidants (2-7). In addition to their biological importance, these ligands are strongly coordinating agents forming complexes with metal ions (8,9).

The benzimidazole derivatives are also important chromophores among organic fluorescent compounds containing aromatic

heterocyclic (10). Essentially the benzimidazole skeleton could be modified in order to enhance their physico-chemical properties.

Besides benzimidazoles, Schiff bases which have great interest due to possess the imine (C=N) group, have potential applications in analytical chemistry and in medicine to cure some diseases as anti-inflammatory, anticancer, antifungal agents (11,12). Schiff base derivatives are also effective molecules used for the optical detection of metal ions due to the presence of the imine group (13).

The design and synthesis of fluorescent sensors which are sensitive to metal ions is a one of the essential research area in chemistry (14). One of the reasons is more advantageous to traditional methods. It is a method that determines easy and inexpensive detection.

A good number of fluorescent receptors have been explored since they have high sensitivity for metal ion (15). Among these, the samples containing benzimidazole unit and Schiff base combination are limited (16, 17).

Development of fluorescent chemosensors capable of selectively determining Zn^{2+} ion has also been an dynamic subject among the studied metal ions recently (18). The Zn^{2+} is a crucial mineral that has an effect on the biological processes in the human body (19). The sensitivity of the sensors is measured by spectroscopically determining changes in their physical properties when encountered with the analyte.

Thus, we report herein the compound **1**, displaying a combination of benzimidazole moiety and bis-aldehyde to form Schiff base derivative that can act as a chemosensor.

We describe the synthesis and characterization of the synthesized benzimidazole-based Schiff base derivative and selectivity towards some cations was studied. The chemosensor behaviors to metal ions (Zn^{+2} , Cd^{+2} , Pb^{2+} , Hg^{+2} , Ba^{2+} and Sb^{3+}) were also studied by absorption and fluorescence spectroscopy.

EXPERIMENTAL

Chemicals and instruments

The following chemicals were obtained from Sigma-Aldrich; 2-hydroxybenzaldehyde, 1,3,5-trioxane, 1,2-phenylenediamine, glycine, hydrochloric acid (HCl), acetic acid (AcOH), sulfuric acid (H_2SO_4), acetonitrile, n-hexane, ethylacetate, dimethylformamide

(DMF), chloroform ($CHCl_3$), methanol (MeOH), ethanol (EtOH), diethyl ether, and K_2CO_3 . All solvents were stored over molecular sieves (4 Å) after they were dried and purified as described by Perrin and Armarego (20). Oxygen-free inert atmosphere was supplied by argon through dual-bank vacuum-gas manifold system. Deionized water was generated from MILLIPORE ultra-pure water supply system. Thin-Layer chromatography (TLC) was performed using silica gel 60-HF254 as an adsorbent. Column chromatography was performed with silica gel (Merck grade 60). Electronic spectra were recorded on a Hitachi U-2900 spectrophotometer with quartz cell of 1 cm. Fluorescence spectra were recorded from Hitachi F-2710 spectrofluorometer. Infrared spectra were acquired on a Perkin Elmer Spectrum two FT-IR spectrometer equipped with Perkin Elmer UATR-TWO diamond ATR and corrected by applying the ATR-correction function of Perkin Elmer Spectrum software. 1H and ^{13}C NMR spectra were recorded a Varian Mercury Plus 300 MHz spectrometer. For MALDI-TOF spectra, the experiments were carried out using a Bruker microTOF (Germany) in Gebze Technical University. 2-aminomethylbenzimidazole dihydrochloride (ambmz·2HCl) and 5,5'-methylenebis(2-hydroxybenzaldehyde) were prepared as described previously (21,22).

Synthesis

(E)-4,4'-methylenebis(2-((E)-(((1H-benzo[d]imidazol-2-yl)methyl)imino)methyl) phenol) (3)

An aqueous solution of ambmz·2HCl (0.78 g, 4.29 mmol in 10 mL) was neutralized by adding aqueous K_2CO_3 solution (0.712 g, 5.2 mmol). A methanolic solution of 5,5'-methylenebis(2-hydroxybenzaldehyde) (0.5 g, 1.95 mmol in 20 mL) was added drop-wise to the above solution with stirring in 1 h. During this period, yellow precipitation slowly formed. The precipitation was then filtered, washed thoroughly with water followed by ethanol/water mixture (1/1) and dried in vacuum. The desired pure compound (**3**) was obtained as a yellow powder in sufficient purity. Yield: 84% (0, 87 g). FT-IR (UATR-TWO™) ν_{max}/cm^{-1} : 3470 (OH), 3366 (NH), 3055-2647 (C-H (Ar) and intermolecular H bonding), 2979-2836 (Aliph., C-H), 1613 (C=N), 1569 (C=C), 1485-1358 (C-C), 1271 (Asym., Ar-O), 1208 (C-N), 1154 (Sym., Ar-O), 789, 748. UV-Vis (DMF): λ_{max} (nm) (log ϵ) 262 (3.56), 294 (3.87), 324 (4.13). 1H -NMR ($CHCl_3$) δ (ppm) : 12.65 (s, 2H), 10.92 (s, 2H), 8.47 (s, 1H), 8.37 (s, 1H), 7.36-7.30 (m, 4H), 7.25-7.20 (m, 2H), 7.17-7.08 (m, 2H), 7.02 (s, 2H), 6.97-6.86 (m, 4H), 5.06 (d, 4H), 3.92 (d, 2H). ^{13}C -NMR ($CHCl_3$) δ (ppm) :

160.50 (C=N), 159.53 (C12), 137.89 (C4), 133.65 (C3), 132.22 (C10), 131.20 (C9), 122.80 (C8), 120.70 (C7), 118.73 (C1), 118.25 (C11), 117.29 (C2), 57.55 (C5), 29.88 (C13). MS (MALDI-TOF): m/z 517.882 [M+1]⁺.

X-Ray Crystal Structure Determination

A suitable single crystal with dimensions 0.55 × 0.44 × 0.24 mm was chosen for the crystallographic study and then carefully mounted on goniometer of a STOE IPDS II diffractometer. Data collection of the title compound, C₈H₁₃Cl₂N₃O, was performed with STOE IPDS II single crystal X-ray diffractometer using graphite monochromated Mo K α radiation ($\lambda = 0.71073 \text{ \AA}$) at room temperature (296 K). Details of the data collection conditions and parameters of refinement process are given in Table 1. Cell parameters were obtained by using X-Area (23) and data reduction was achieved with X-RED32 (23) software. The maximum peaks and deepest hole observed in the final $\Delta\rho$ map were 0.77 and -0.39 e \AA^{-3} , respectively. The scattering factors were taken from SHELXL-97 (24). The molecular graphics were done using ORTEP-3 for Windows (25). All non-hydrogen

atoms were refined anisotropically. H atoms were positioned geometrically, with N-H = 0.86 \AA (for NH and NH₃) and C-H = 0.93 \AA for aromatic H, respectively, and constrained to ride on their parent atoms, with Uiso(H) = 1.2Ueq(C,N). The coordinates of the H atoms of the water molecule were determined from a difference Fourier map and refined isotropically subject to a restraint of O-H = 0.82 \AA . The general-purpose crystallographic tool PLATON (26) was used for the structure analysis. WinGX (27) was used to prepare the data for publication. Details of the data collection conditions and the parameters of refinement process are given in Table 1.

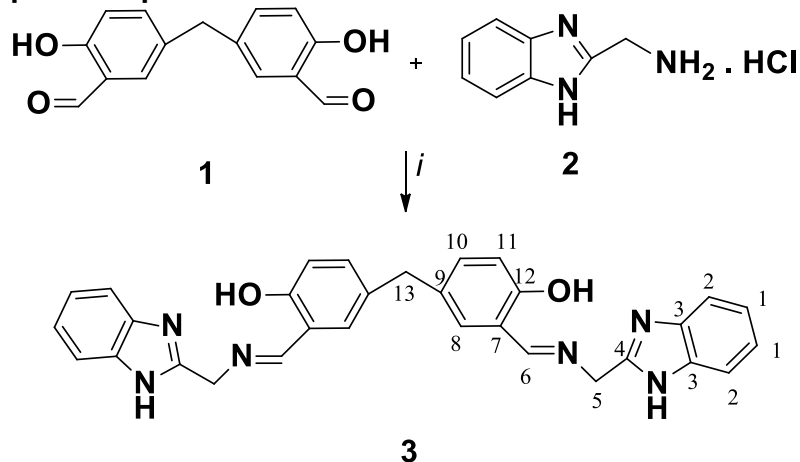
CCDC 1474738 contains supplementary crystallographic data (excluding structure factors) for the compound reported in this article. These data can be obtained free of charge via <http://www.ccdc.cam.ac.uk/deposit> [or from the Cambridge Crystallographic Data Center (CCDC), 12 Union Road, Cambridge CB2 1EZ, UK; fax: +44(0)1223 336033; e-mail: deposit@ccdc.cam.ac.uk].

Table 1. Crystallographic data and refinement parameters for the compound, C₈H₁₃Cl₂N₃O

| | |
|---|--|
| Crystal data | |
| Chemical moiety formula | C ₈ H ₁₁ N ₃ ²⁺ ·2(Cl ¹⁻)·H ₂ O |
| Chemical sum formula | C ₈ H ₁₃ Cl ₂ N ₃ O |
| <i>M_r</i> | 238.11 |
| Crystal system, space group | Monoclinic, <i>P</i> 2 ₁ / <i>c</i> |
| Temperature (K) | 296 |
| <i>a</i> , <i>b</i> , <i>c</i> (\AA) | 6.9580 (3), 12.1395 (6), 25.1958 (11) |
| β ($^\circ$) | 90.402 (4) |
| <i>V</i> (\AA^3) | 2128.15 (17) |
| <i>Z</i> | 8 |
| Radiation type | Mo <i>K</i> α |
| μ (mm^{-1}) | 0.58 |
| Crystal size (mm) | 0.55 × 0.44 × 0.24 |
| Data collection | |
| Diffractometer | STOE IPDS 2 |
| Absorption correction | Integration <i>X-RED32</i> (Stoe & Cie, 2002) |
| <i>T_{min}</i> , <i>T_{max}</i> | 0.730, 0.897 |
| No. of measured, independent and observed [<i>I</i> > 2 σ (<i>I</i>)] reflections | 13266, 4405, 2254 |
| <i>R_{int}</i> | 0.123 |
| ($\sin \theta/\lambda$) _{max} (\AA^{-1}) | 0.628 |
| Refinement | |
| <i>R</i> [<i>F</i> ² > 2 σ (<i>F</i> ²)], <i>wR</i> (<i>F</i> ²), <i>S</i> | 0.067, 0.164, 0.84 |
| H-atom treatment | H atoms treated by a mixture of independent and constrained refinement |
| $\Delta\rho_{\text{max}}$, $\Delta\rho_{\text{min}}$ (e \AA^{-3}) | 0.77, -0.39 |

RESULT AND DISCUSSION

Synthesis and spectroscopic characterization



Scheme 1. Synthesis of target compound: (i) K_2CO_3 , water, methanol.

As a first step, 5,5'-methylenebis(2-hydroxybenzaldehyde) (**1**) was obtained with the reaction of salicylaldehyde and 1,3,5-trioxane in the presence of a mixture of conc. H_2SO_4 and AcOH in good yield according to the reported literature (21). The reaction of the other precursor (**2**) was conducted in 5.5 M HCl with the condensation reaction of glycine and 1,2-phenylenediamine (22).

The new bis-Schiff-base ligand (**3**) was synthesized by Schiff-base condensation as stated in Scheme 1. 5,5'-methylenebis(2-hydroxybenzaldehyde) (**1**) reacted with 2-aminomethylbenzimidazole dihydrochloride (ambmz·2HCl) in methanol/water in the presence of K_2CO_3 for neutralization to afford the product **3**. The expected chemical structure was proved by spectroscopic methods such as FT-IR, 1H -NMR, ^{13}C -NMR and MS analysis. The analysis results confirmed the expected structure.

When the FT-IR spectrum is evaluated comparatively, the carbonyl vibration at 1655 cm^{-1} and the C-H vibrations of aldehyde group at 2857 cm^{-1} and 2743 cm^{-1} arising from **1** were disappeared after the conversion completed to give **3**. Formation of benzimidazole-based Schiff base was also supported by the appearance of imine band at 1613 cm^{-1} and -NH stretching at 3366 cm^{-1} that the condensation reaction occurred to give **3**.

The electronic absorption spectra of **1** and **3** in DMF are shown in Figure 1. 5,5'-methylenebis(2-hydroxybenzaldehyde) (**1**) presented two absorptions at 266 and 332 nm in DMF in the UV-Vis spectrum. The UV-Vis spectrum of **3** showed three absorption maxima at 262, 294 and 324 nm. The observed broad maximum at 345 nm could be attributed to the $n\text{-}\pi^*$ transition of the azomethine group while the bands at 262 and 294 nm refer to the $\pi\text{-}\pi^*$ transitions in the UV-Vis spectrum of **3** (28).

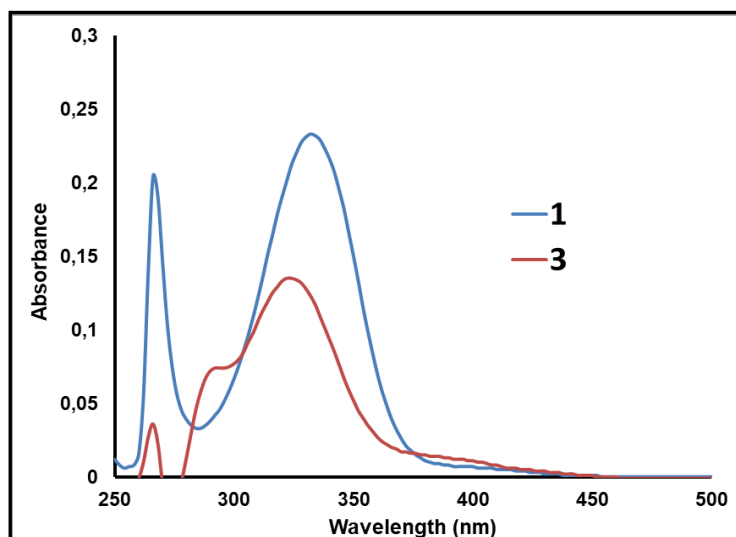


Figure 1. UV-Vis spectra of **1** and **3** in DMF. (Concentration 1×10^{-5} mol.L $^{-1}$)

The $^1\text{H-NMR}$ data provided sufficient information for characterization of the target structure (**3**). When compared the $^1\text{H-NMR}$ spectra of compound **1** and **3**, the disappearances of HC=O proton signal of 5,5'-methylenebis(2-hydroxybenzaldehyde) (**1**) and the appearance of new peaks in aromatic region at 8.47 ppm and 8.37 ppm belongs to the imine protons and the $-\text{NH}$ peak at 10.92 ppm shows that the imine condensation reaction has occurred. The other characteristic peak was observed at 5.06 ppm related to methylene group of the benzimidazole unit (in supporting information).

In the $^{13}\text{C-NMR}$ spectrum of **3** the presence of the peaks at 160.50 ppm and 159.53 ppm are attributed to the carbon atoms of the imine are the obvious differences from **1**. For the $^{13}\text{C-NMR}$ spectrum of **3**, the carbon atom arising from methylene group of benzimidazole was observed at 57.55 ppm (in supporting information).

The mass spectrum of **3** confirmed the expected structure with the result obtained from MALDI-TOF Mass spectrometer. The mass spectrum of **3** gave the molecular ion peaks at m/z : 517.882 $[\text{M}+1]^+$ clearly illustrating the formation of final compound.

Description of the crystal structures

The ORTEP diagram of the crystal structure, 2-(ammoniomethyl)-1H-benzimidazol-3-ium chloride hydrate, $\text{C}_8\text{H}_{13}\text{Cl}_2\text{N}_3\text{O}$ with thermal ellipsoids drawn at a 40% probability is shown in Figure 2.

The experimental geometric parameters and hydrogen bonding given in Tables 1 and 2, respectively. The molecular structure of the title compound is illustrated in Fig. 1. The asymmetric unit of ' $\text{C}_8\text{H}_{13}\text{Cl}_2\text{N}_3\text{O}$ ' contains one ($\text{O-H}\cdots\text{Cl}$), two ($\text{N-H}\cdots\text{O}$) and five ($\text{N-H}\cdots\text{Cl}$) intramolecular hydrogen bonds (Figure 2).

Table 2. Hydrogen bond properties (\AA , $^\circ$) for $\text{C}_8\text{H}_{13}\text{Cl}_2\text{N}_3\text{O}$.

| $D-H\cdots A$ | $D-H$ | $H\cdots A$ | $D\cdots A$ | $D-H\cdots A$ |
|---|----------|-------------|-------------|---------------|
| $\text{N3}-\text{H3B}\cdots\text{Cl4}^{\text{i}}$ | 0.87 (2) | 2.46 (3) | 3.282 (5) | 156 (4) |
| $\text{N3}-\text{H3A}\cdots\text{Cl1}^{\text{ii}}$ | 0.87 (2) | 2.27 (2) | 3.130 (5) | 170 (5) |
| $\text{N3}-\text{H3C}\cdots\text{Cl3}$ | 0.87 (2) | 2.33 (4) | 3.111 (5) | 149 (5) |
| $\text{N6}-\text{H6A}\cdots\text{Cl4}$ | 0.87 (2) | 2.24 (2) | 3.113 (5) | 176 (5) |
| $\text{N6}-\text{H6C}\cdots\text{Cl1}^{\text{iii}}$ | 0.88 (2) | 2.41 (2) | 3.265 (4) | 165 (4) |
| $\text{N6}-\text{H6B}\cdots\text{Cl2}$ | 0.86 (2) | 2.32 (3) | 3.111 (5) | 152 (5) |
| $\text{O1}-\text{H1A}\cdots\text{Cl2}$ | 0.84 (2) | 2.29 (2) | 3.131 (4) | 171 (6) |
| $\text{O2}-\text{H2A}\cdots\text{Cl3}$ | 0.84 (2) | 2.36 (3) | 3.157 (4) | 160 (6) |
| $\text{N2}-\text{H2C}\cdots\text{Cl1}$ | 0.85 (2) | 2.28 (2) | 3.101 (4) | 161 (4) |
| $\text{N1}-\text{H1C}\cdots\text{O1}$ | 0.85 (2) | 1.94 (3) | 2.755 (5) | 161 (6) |
| $\text{N4}-\text{H4A}\cdots\text{O2}$ | 0.86 (2) | 1.90 (2) | 2.753 (5) | 171 (5) |
| $\text{N5}-\text{H5A}\cdots\text{Cl4}^{\text{iv}}$ | 0.84 (2) | 2.30 (2) | 3.141 (4) | 173 (4) |

Symmetry codes: (i) $x+1, y, z$; (ii) $-x+2, y-1/2, -z+3/2$; (iii) $-x+1, y-1/2, -z+3/2$; (iv) $-x, -y+1, -z+1$.

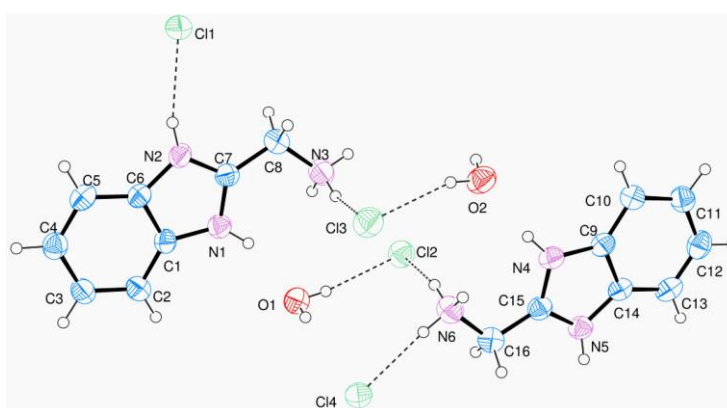


Figure 2. ORTEP plot of the $\text{C}_8\text{H}_{13}\text{Cl}_2\text{N}_3\text{O}$. View of the title compound, with displacement ellipsoids for non-H atoms drawn at the 40% probability level. The intramolecular hydrogen bond for asymmetric unit is shown as a dashed line.

The r.m.s. departure of the molecule's benzimidazolium rings are 0.0071 \AA for $\text{N1/C1/C2/C3/C4/C5/C6/N2/C7}$ (ring1), 0.0108 \AA for $\text{N4/C9/C10/C11/C12/C13/C14/N5/C15}$ (ring2). The dihedral angle between benzimidazolium rings (ring1/ring2) is 1.156 (0.128) $^\circ$. These benzimidazolium rings are almost planar. The maximum deviation of the ring1 ring2 from planarity is -0.014 (3) \AA for atom C7, 0.016 (1) \AA for atom, respectively. The aromatic C-C distances for ring1 and ring 2 range from 1.3754(1) \AA to 1.4145(1) \AA and

from 1.3626(1) \AA to 1.4040(1) \AA , respectively. Geometric structure of all benzimidazolium rings is the same; particularly, the C7-N1 bond length is identical to the C15-N4 length [mean = 1.332 (5) \AA], while the C7-N2, C15-N5 lengths are also not significantly different [mean = 1.337 (2) \AA]. These values are consistent with the C7-N1 and C15-N4 bonds possessing more double-bond character than the C7-N2 and C15-N5 bonds (Table 3). This obtained bonds length is in a good accordance with previously reported values by Zheng *et al.* (29), Cui (30) and Li *et al.* (31).

Table 3. Selected bond lengths (\AA) and angles ($^\circ$) for $\text{C}_8\text{H}_{13}\text{Cl}_2\text{N}_3\text{O}$

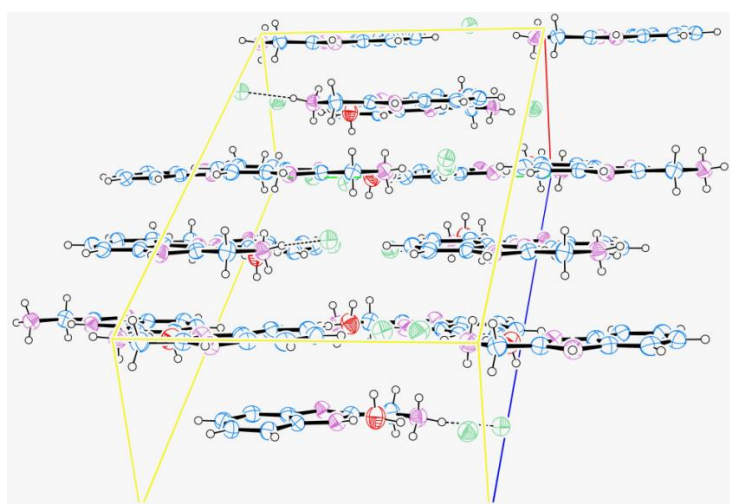
| Bond lengths (\AA) | | | |
|---|------------|---|-----------|
| $\text{N2}-\text{C7}$ | 1.334 (5) | $\text{N3}-\text{C8}$ | 1.447 (6) |
| $\text{N5}-\text{C15}$ | 1.340 (5) | $\text{N6}-\text{C16}$ | 1.446 (6) |
| $\text{N1}-\text{C7}$ | 1.332 (5) | $\text{C15}-\text{C16}$ | 1.482 (6) |
| $\text{N4}-\text{C15}$ | 1.332 (5) | | |
| Bond angles ($^\circ$) | | | |
| $\text{N1}-\text{C7}-\text{C8}$ | 128.2 (4) | $\text{N5}-\text{C15}-\text{C16}$ | 123.4 (4) |
| $\text{N2}-\text{C7}-\text{C8}$ | 122.8 (3) | $\text{N6}-\text{C16}-\text{C15}$ | 113.5 (4) |
| $\text{N4}-\text{C15}-\text{C16}$ | 127.0 (4) | $\text{N3}-\text{C8}-\text{C7}$ | 112.7 (4) |
| Torsion angles ($^\circ$) | | | |
| $\text{C1}-\text{N1}-\text{C7}-\text{C8}$ | -175.7 (4) | $\text{N4}-\text{C15}-\text{C16}-\text{N6}$ | 5.3 (7) |

| | | | |
|----------------|------------|---------------|------------|
| C6—N2—C7—C8 | 175.9 (4) | N5—C15—C16—N6 | -178.2 (4) |
| C9—N4—C15—C16 | 175.6 (4) | N1—C7—C8—N3 | -6.1 (7) |
| C14—N5—C15—C16 | -176.1 (4) | N2—C7—C8—N3 | 176.6 (4) |

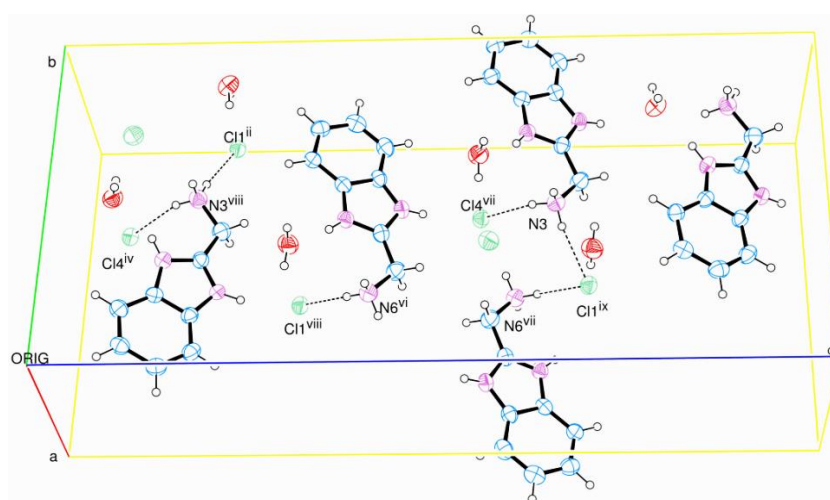
The crystal stacking of studied composite is stabilized by intramolecular hydrogen bonds, [(O—H...Cl), (N—H...O), (N—H...Cl)], intermolecular hydrogen bonds, (N—H...Cl) and intermolecular π - π stacking interactions between C1-C6 phenyl rings and C1/N1/C7/N2/C6 imidazole rings (Table 2, Figure 2 and Figure 3).

Two O atoms and six N atoms of the compound include hydrogen bonds, as shown in Table 2. The 1H-benzoimidazole cation adopts a planar conformation with an rms deviation of 0.0108 Å for the fitted atoms. The cation and anion in the asymmetric unit are linked by N6—H6B...Cl2, N1—H1C...O1 and O1—H1A...Cl2 hydrogen bonds. Among two cationic ethanaminium groups (NH₃⁺) and two Cl⁻ anions of compound are assembled into a dimer via these hydrogen bonds. The crystal stacking is further stabilized by intermolecular π ... π packing interactions {between [the C1-

C6 (ring 3)/C9-C14 (ring 4) phenyl rings (symmetry code: x, y, z) of neighboring anions with centroid-to-centroid distances, 3.3462 (2) Å}, [the N1/C1/C6/N2/C7 (ring 5) imidazolium/ring 4 (symmetry code: $1+x, y, z$) of neighboring cations with centroid-to-centroid distances, 3.5309 (2) Å] and [the N4/C9/C14/N5/C15 (ring 6) imidazolium/ring 3 (symmetry code: $1+x, y, z$) of neighbouring cations with centroid-to-centroid distances, 3.5527 (2) Å]}, respectively.



(a)



(b)

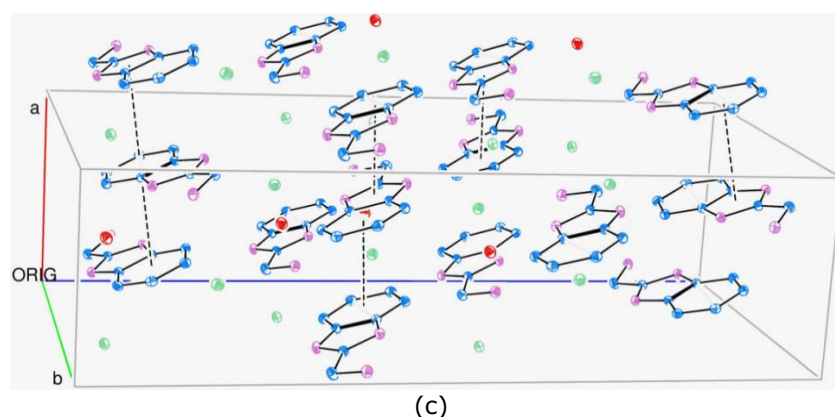


Figure 3. (a) Crystal-packing diagram of the title compound, $C_8H_{13}Cl_2N_3O$. (b) A view showing the hydrogen-bonded chains throughout the c axis. (c) A view showing the π - π stacking interaction chains throughout the a axis. π - π interactions with dashed lines are shown.

Spectroscopic studies of **3** toward Zn^{2+}

The affinity of the chemosensor **3** toward different metal ions (Zn^{2+} , Cd^{2+} , Pb^{2+} , Hg^{2+} , Ba^{2+} and Sb^{3+}) was monitored using UV-visible and fluorescence spectroscopy. All the spectral measurements were carried out in DMF solutions ($C=1.0 \times 10^{-5}$ M) of **3**. The binding affinity experiments were performed by maintaining the ligand concentration and changing the molar ratio of the added metal ion at room temperature.

The spectra were obtained at 25 °C in a 3 mL volume cuvette by adding increasing amounts of metal ion solutions. The metal ions studied were Zn^{2+} , Cd^{2+} , Pb^{2+} , Hg^{2+} as their acetate salts, Ba^{2+} and Sb^{3+} as their nitrate and chloride salts, respectively.

The ligand **3** did not form complexes with Cd^{2+} , Pb^{2+} , Hg^{2+} , Ba^{2+} , and Sb^{3+} ions. However, when the prepared solution of ligand (**3**) is treated with a solution containing Zn^{2+} ion, the absorption spectrum of ligand **3** illustrated selectivity towards to the Zn^{2+} ion as represented in Figure 4. In case of adding Zn^{2+} solution to the Schiff base derivative (**3**), a decrease was observed in the band at 324 nm while an increment was observed at 262 and 374 nm absorbance. Besides, the observed band at 324 nm which is associated with the free ligand (**3**) shifted to 374 nm after mixing with the solution of the Zn^{2+} and this shifting is indicative for the coordination of Zn^{2+} to the **3** upon complexation (32).

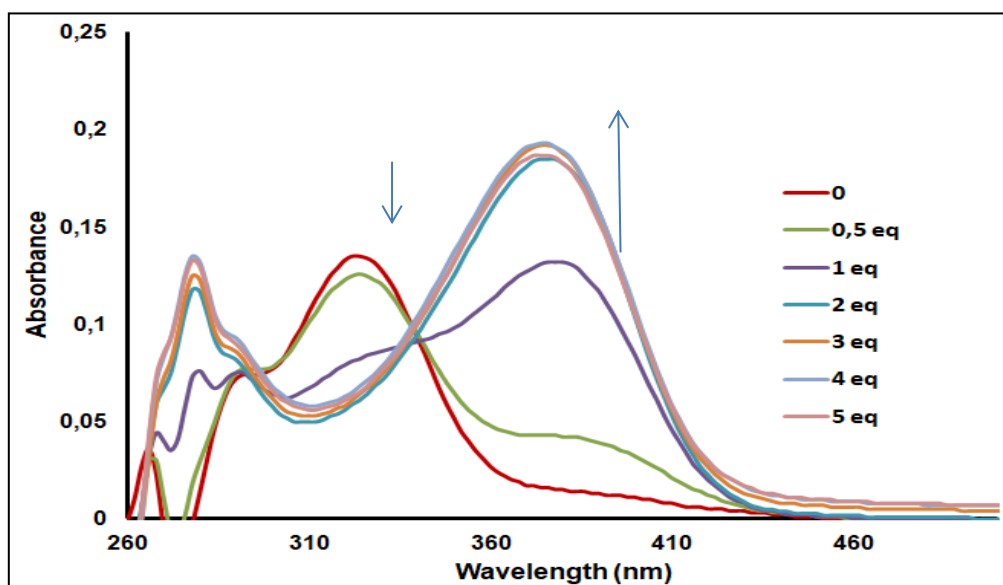


Figure 4. UV-Vis spectra of **3** (1×10^{-5} mol L^{-1}) with different amount of Zn^{2+} .

Investigations of fluorescent behavior of **3** for the various metal ions are as shown in Figure

5. Significant changes in fluorescent emission intensity were not observed in low upon

addition of the cations (Cd^{2+} , Pb^{2+} , Hg^{2+} , Ba^{2+} and Sb^{3+}) except for Zn^{2+} .

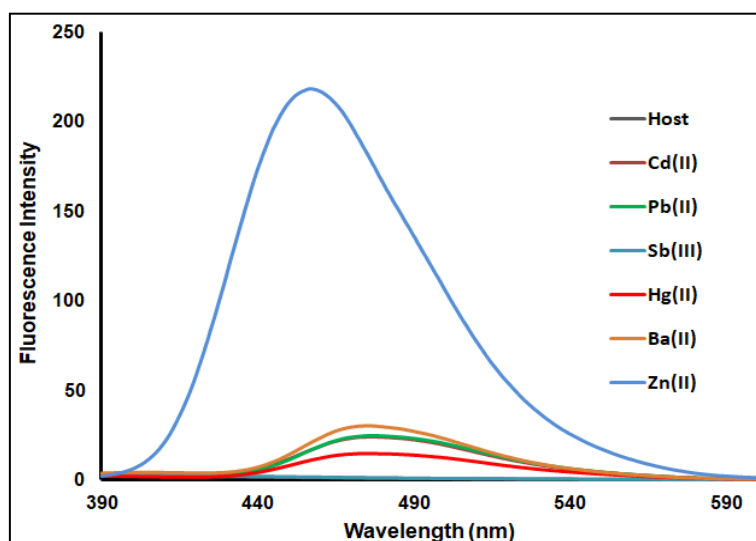


Figure 5. Emission spectra of **3** (1×10^{-5} M) in the presence of Zn^{2+} , Pb^{2+} , Hg^{2+} , Cd^{2+} , Ba^{2+} , Sb^{3+} (12×10^{-8} M) in DMF at 25°C ($\lambda_{\text{exc}} = 378$ nm).

After Schiff base (**3**) was treated with different concentrations of Zn^{2+} , the observed fluorescence emission at about 450 nm were plotted by exciting from two different wavelengths as 324 nm (Figure 6) and 378 nm (Figure 7).

Compound **3** alone exhibits weak fluorescence emission at about 383 nm when it was excited at 324 nm in DMF. After titration with Zn^{2+} , the emission intensity was dramatically increased and showed red shift to 450 nm (Figure 6).

When the fluorescence titration experiments were performed by exciting at about 378 nm which is the absorption wavelength of the formed complex, a significant enhancement at fluorescence emission intensity was observed (Figure 7). The increment of the fluorescent emission could be explained with the occurrence of a rigid metal complex system after binding of Zn^{2+} ion (18). It is clear that these significant spectral changes indicate the high selectivity of **3** for the Zn^{2+} (Figure 6-7).

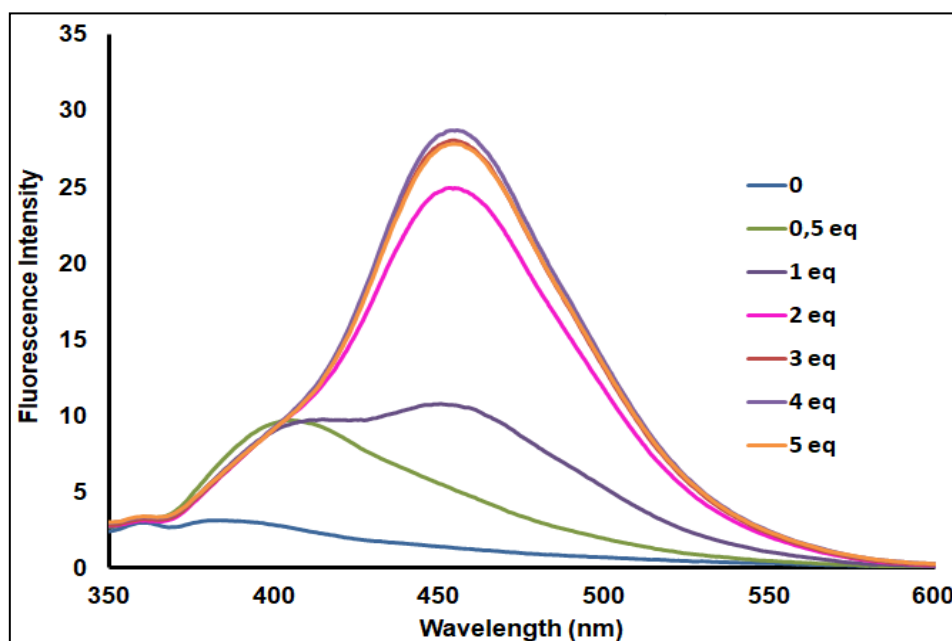


Figure 6. Emission spectra of **3** (1×10^{-5} M) in the presence of increasing amounts of Zn^{2+} in DMF at 25°C ($\lambda_{\text{exc}} = 324$ nm).

In addition to spectral changes, the color of the ligand solution turned to fluorescent blue as a response to Zn^{2+} metal ions which is clear under visible light. The addition of other metal ions did not make a significant change in the fluorescence emission and in the color of the

ligand solution. The observed bright blue reflection was provided only at $\mathbf{3} + Zn^{2+}$ composition under UV-light. The image obtained at the beginning and end of the measurement is as shown in the graph as embedded in Figure 7.

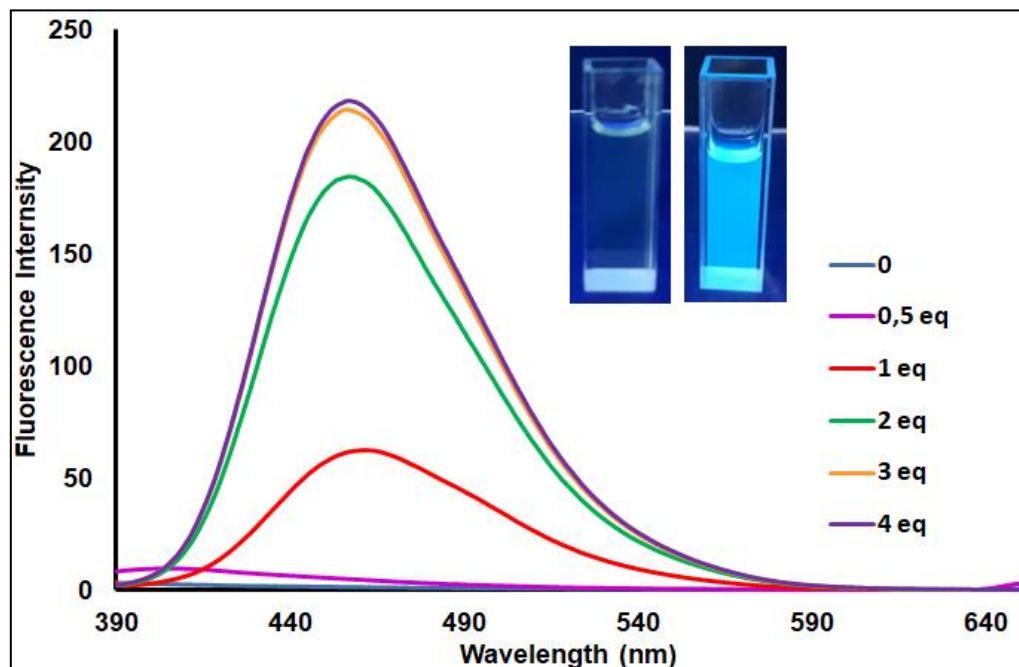


Figure 7. Emission spectra of $\mathbf{3}$ (1×10^{-5} M) in the presence of increasing amounts of Zn^{2+} in DMF at $25^\circ C$ ($\lambda_{exc} = 378$ nm).

Fluorescence Spectra and Fluorescence quantum yields

The quantum yields of fluorescence were obtained using the following equation 1 (33),

$$\Phi_F = \Phi_F(\text{Std}) \frac{F \cdot A_{\text{Std}} \cdot n^2}{F_{\text{Std}} \cdot A \cdot n_{\text{Std}}^2} \quad (\text{Eq. 1})$$

F and F_{Std} symbolize the areas under the emission curves of the sample and the standard, respectively (34). A and A_{Std} are the absorbances at the excitation wavelengths of the samples and standard, respectively.

n^2 and n_{Std}^2 are the refractive indices of solvents which used in experiment for the samples and

standard, respectively. ($\eta_{\text{chloroform}}:1.445$, $\eta_{\text{DMSO}}:1.480$, $\eta_{\text{DMF}}:1.430$)

The fluorescence emission spectra of newly synthesized compound $\mathbf{3}$ were studied in DMSO and DMF and $CHCl_3$ at 1×10^{-5} M at the room temperature and the spectra were given in (Figure 8). The peaks of fluorescence emission were observed at: 326 nm in $CHCl_3$, 329 nm in DMF and 330 nm in DMSO for $\mathbf{3}$. The quantum yield values of fluorescence (Φ_F) were found 0.001 in $CHCl_3$, 0.05 in DMF and 0.175 in DMSO for $\mathbf{3}$, respectively. Comparing these results, the highest value obtained in DMSO and the yields in all solvents are lower than the quantum yield of standard naphthalene (0.23) in cyclohexane.

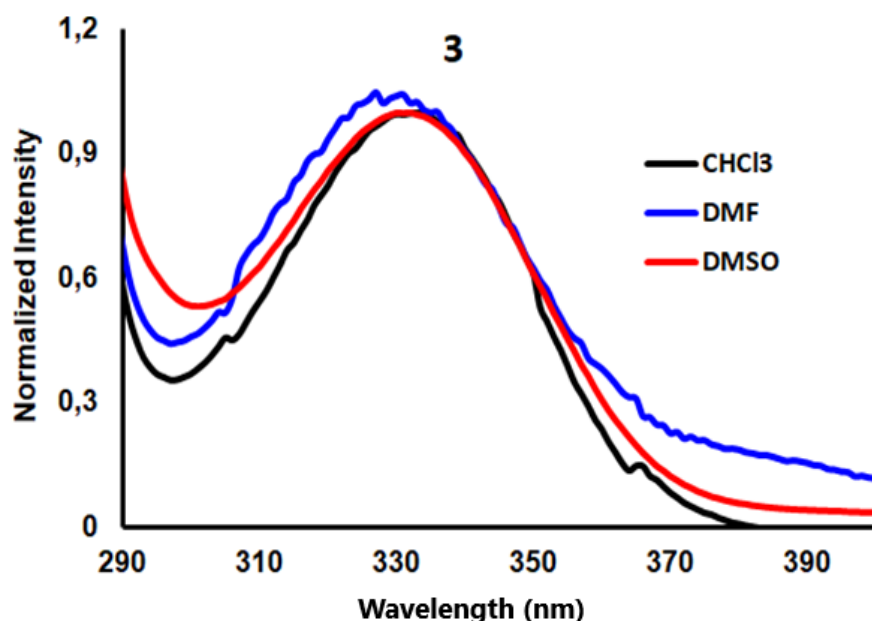


Figure 8. Normalized Emission spectra of **3** in CHCl_3 , DMF and DMSO.

CONCLUSION

In this study, a new Schiff base derivative **3** was reported for the first time. The characterization of compound (**3**) was confirmed with the spectroscopic methods. We wanted to define a new type of molecule formed by the combination of two functional compounds which are benzimidazole unit and Schiff base, with a small number in the literature. In addition to the introduction of a new molecule to the literature, we examined the sensor behavior of this new molecule. The most possible binding mode of the complex of **3** coordinated with different cations was studied based on the absorption spectra and fluorimetric titration experiments. The newly synthesized benzimidazole based-Schiff base derivative showed highly selectivity toward Zn^{2+} ions among the metal ions examined in DMF. Absorption and fluorimetric titration experiments exhibited that the newly synthesized compound (**3**) could be utilized as chemosensors for detection of Zn^{2+} ion.

ACKNOWLEDGMENTS

This work was supported by Research Fund of Sakarya University (project no. 2014-02-04 007).

REFERENCES

- Preston PN. Chemistry of Heterocyclic Compounds: Benzimidazoles and Cogeneric Tricyclic Compounds. John Wiley&Sons, Inc, New York; 2008
- El Rashedy AA, Aboul-Enein HY. Benzimidazole derivatives as potential anticancer agents. *Mini-Rev. Med. Chem.* 2013;13:399-407.
- El-masry AH, Fahmy HH, Abdelwahed SH. Synthesis and Antimicrobial Activity of Some New Benzimidazole Derivatives. *Molecules.* 2000;5:1429-38.
- Gaba M, Singh S, Mohan C. Benzimidazole: An emerging scaffold for analgesic and anti-inflammatory agents. *Eur. J. Med. Chem.* 2014;76:494-505.
- Patil A, Ganguly S, Surana S. A systematic Review of benzimidazole Derivatives as an Antiulcer Agent. *Rasayan J Chem.* 2008;1:447-60.
- Kus C, Kilcgil AG, Eke BC, Iscan M. Synthesis and antioxidant properties of some novel benzimidazole derivatives on lipid peroxidation in the rat liver. *Arch Pharm. Res.* 2004;27:156-63.
- Kathiravan MK, Salake AB, Chothe AS, Dudhe PB, Wat RP. The biology and chemistry of antifungal agents: A review. *Bioorg Med. Chem.* 2012;20:5678-98.
- Cetinkaya B, Özdemir I, Bruneau C, Dixneuf PH. Benzimidazole, Benzothiazole and Benzoxazole Ruthenium(II) Complexes; Catalytic Synthesis of 2,3-Dimethylfuran. *Eur J Inorg. Chem.* 2000;2000:29-32.
- Tong Y, Zheng S, Chen X. Structures, Photoluminescence and Theoretical Studies of Two Zn^{II} Complexes with Substituted 2-(2-

- Hydroxyphenyl)benzimidazoles. *Eur J Inorg Chem.* 2005;2005:3734-41.
10. Verdasco G, Martin MA, Castillo B, Lopez-Alvarado P, Menendez JC. Solvent effects on the fluorescent emission of some new benzimidazole derivatives. *Anal Chim Acta.* 1995;303:73-8.
11. Arulmurugan S, Kavitha HP, Venkatraman BR. Biological Activities of Schiff Bae and Its Complexes: A Review. *Rasayan J Chem.* 2010;3: 385-410.
12. Przybylski P, Huczynski A, Pyta K, Brzezinski B, Bartl F. Biological Properties of Schiff Bases and Azo Derivatives of Phenols. *Curr Org. Chem.* 2009;13:124-48.
13. Wang L, Qin W, Liu W. A sensitive Schiff-base fluorescent indicator for the detection of Zn^{2+} . *Inorg Chem Commun.* 2010;13:1122-25.
14. Silva AP, Gunaratne HQN, Gunnlaugsson T, Huxley AJM, McCoy CP, Rademacher JT, Rice TE, Signaling Recognition Events with Fluorescent Sensors and Switches. *Chem Rev.* 1997;97:1515-66.
15. Carter KP, Young AM, Palmer AE. Fluorescent Sensors for Measuring Metal Ions in Living Systems *Chem Rev.* 2014;114: 4564-4601.
16. Singh N, Jang DO. Benzimidazole-Based Tripodal Receptor: Highly Selective Fluorescent Chemosensor for Iodide in Aqueous Solution. *Org Lett.* 2007;9:1991-4.
17. Lee DY, Singh N, Jang DO. A benzimidazole-based single molecular multianalyte fluorescent probe for the simultaneous analysis of Cu^{2+} and Fe^{3+} . *Tetrahedron Lett.* 2010;51:1103-6.
18. Lin H, Cheng P, Wanb C, Wu A, A turn-on and reversible fluorescence sensor for zinc ion. *Analyst.* 2012;137: 4415-7.
19. Auld DS. Zinc coordination sphere in biochemical zinc sites. *BioMetals.* 2001;14:271.
20. Perrin DD, Armarego WLF, Perrin DR. Purification of Laboratory Chemicals. Pergamon Press, New York:2013.
21. Lin CH, Feng YR, Dai KH, Chang HC, Juang TY. Synthesis of a benzoxazine with precisely two phenolic OH linkages and the properties of its high-performance copolymers. *J Polym Sci Part A: Polym Chem.* 2013;51:2686-94.
22. Alasmay FAS, Snelling AM, Zain ME, Alafeefy AM, Awaad AS, Karodia N. *Molecules.* 2015;20:15206-23.
23. STOE & Cie, X-Area (Version 1.18) and X-RED32 (Version 1.04), STOE & Cie, Darmstadt, Germany;2002.
24. Sheldrick GM. A short history of SHELX. *Acta Crystallogr., Sect. A: Found. Crystallogr.* 2008;64:112-122.
25. Farrugia LJ. ORTEP-3 for Windows- a version of ORTEP-III with a Graphical User Interface (GUI). *J Appl Crystallogr.* 1997;30:565.
26. Spek AL. Structure validation in chemical crystallography. *Acta Crystallogr.* 2009;D65:148-55.
27. Farrugia LJ. WinGX and ORTEP for Windows: an update. *J Appl Crystallogr.* 1999;32:837-838.
28. Özçelik S, Gül A. Boronic ester of a phthalocyanine precursor with a salicylaldimino moiety. *J Organomet. Chem.* 2012;699:87-91.
29. Zheng S, Cai Y, Zhanga X, Sua C. 2,2'-(Iminodimethylene)bis(1H-benzimidazolium)(1+) chloride. *Acta Cryst.* 2005;E61:642-4.
30. Cui Y. 2,2',2''-(Nitrilotrimethylene)tris(1Hbenzimidazol-3-ium) trinitrate. *Acta Cryst.* 2011;E67:625-6.
31. Li G, Yang F, Yao C. 2-Amino-1H-benzimidazol-3-ium 4,4,4-trifluoro-1,3-dioxo-1-phenylbutan-2-ide. *Acta Cryst.* 2008;E64:2460.
32. Jana A, Sukul PK, Mandal SK, Konar S, Ray S, Das K, et al. A novel 2,6-diformyl-4-methylphenol based chemosensor for Zn(II) ions by ratiometric displacement of Cd(II) ions and its application for cell imaging on human melanoma cancer cells. *Analyst,* 2014;139:495-504.
33. Sen P, Atmaca GY, Erdogmus A, Dege N, Genc H, Atalay Y, Yildiz SZ. The Synthesis, Characterization, Crystal Structure and Photophysical Properties of a New Meso-BODIPY Substituted Phthalonitrile. *J Fluoresc.* 2015;25:1225-34.
34. Brouwer AM. Standards for photoluminescence quantum yield measurements in solution (IUPAC Technical Report). *Pure Appl Chem.* 2011;83:2213-28.